TECHNICAL TRANSACTIONS | CZASOPISMO TECHNICZNE
CIVIL ENGINEERING | BUDOWNICTWO
3-B/2016
DOI: 10.4467/2353737XCT.16.216.5965

BARBARA KOŻUCH, TADEUSZ TATARA*

SELECTED RESULTS OF VIBRATIONS PROPAGATION IN GROUND SUBSURFACE LAYERS CAUSED BY TRAIN RUNS

WYBRANE WYNIKI PROPAGACJI DRGAŃ W WARSTWACH PRZYPOWIERZCHNIOWYCH GRUNTU OD PRZEJAZDÓW POCIĄGÓW

Abstract

The study presents a selection of free-field vibration measurement results (the horizontal component *x* vibration is perpendicular to the axis of the track) in the ground surface layer, in one of the three measuring polygons. Pendolino, InterCity and InterRegio trains, excited free-field vibrations. Results for speeds of 120 and 160 km/h were analysed to have comparison that is more tangible.

Keywords: trains, free-field vibration, propagation

Streszczenie

W pracy przedstawia się wybrane wyniki pomiarów drgań gruntu (składowa pozioma x drgań prostopadła do osi toru) w przypowierzchniowej warstwie, w jednym z trzech poligonów pomiarowych. Drgania gruntu wzbudzane były przejazdami pociągu Pendolino i składów InterCity oraz InterRegio. W celach porównawczych analizuje się przejazdy z prędkościami 120 i 160 km/h.

Słowa kluczowe: pociągi, drgania gruntu, propagacja

* M.Sc. Eng. Barbara Kożuch, Prof. Ph.D. D.Sc. Tadeusz Tatara, Faculty of Civil Engineering, Cracow University of Technology.

1. Introduction

In November of 2013, homologation and velocity tests took place. One of the twenty newly purchased Pendolino trains (Electric Multiple Unit – EMUs 250) was crossing the Psary–Góra Włodowska section (approximately 36 km) located within the Central Rail Line (CRL) No. 4. Electric Multiple Unit was running with dedicated speeds. Parameters such as acceleration and displacement of rails, mechanical vibrations of individual elements of railway tracks and noise were measured. Geotechnical conditions in the surroundings of the railway line were also analysed. Measurements were carried out during three weekends in November. The train was following the first track with two tracks closed for other vehicles. During weekdays, similar studies were done for vehicles running the (CRL) section. Similar studies were mentioned in paper [1].

The paper presents selected results of measurements of free-field vibration (horizontal component of vibration (x) – perpendicular to the axis of the track) in the surface layer, in one of the three measuring polygons. Passages of the Pendolino (EMU 250), the InterCity and the InterRegio trains induced free-field vibrations. The data from the trains' runs at a speed of 120 and 160 km/h is a basis for comparison.

The staff of an accredited Laboratory of Structural Mechanics at the Cracow University of Technology (Accreditation No. AB 826) conducted vibration measurements.

The analysis was performed based on the knowledge and experience of the research team, and it is also available in the references [2–4].

2. Measuring polygon

During research, ground conditions were also monitored to check if they have any significant influence on the propagation of vibrations.

In the cross-examination, measurements of the soil properties were carried out at two places (at the foot of the railway embankment and at a distance of 20 m) located near the points at which the attachment sensors (accelerometers) measured free-field vibrations. Fig. 1 shows a cross-section of a geological lithographic profile.

Based on the properties of the ground, it turned out that the substrate is layered. In the profile under a thin layer of humus soil consists of natural coarse and incohesive (sand, sandy silt with depth in the passing sands with gravels, drilled a single interbeddings powder) layers. In the audited profile, there was no groundwater. On this basis, it was concluded that the ground is in the vadose zone. The tested soil was humid [5, 6].

Free-field vibration measurements were made with piezoelectric accelerometers' PCB Piezotronics and the SCADAS Mobile's LMS International analyser. The relative standard uncertainty of the maximum signal acceleration must not exceed ± 11.61%, which is the sum of the deviations of nominal sensors and amplifier distortion by the digital recorder and the accuracy as well as the linearity of the amplifier. In the test, profile arrangement of sensors is shown in Figure 2. Seven sensors recording the horizontal vibrations perpendicular to the axis were arranged sequentially – first under the railway embankment, further every ten meters in a direction perpendicular to the axis. Accelerometers were fixed on the ground, 2.3 m below the rail. Mounting the sensor on the base was carried out according to the method described in [7, 8].

Stratygraphy		Lithological profile	Depth	Lithological profile	Soil symbol
Quaternary	Holocene	0	0.00	Brown soil	Gb
			0.10	Medium sand with an admixture of gravel brownish yellow	grMSa
			0.60	Medium sand with powder brownish yellow	siMSa
			0.70	Powder light brown	siMSa
		1	1.00	Medium sand with fine sand dark yellow	fsaMSa
		2	2.18	Medium sand with powder brownish yellow	siMSa
			2.56	Medium sand with fine sand dark yellow	fsaMSa
			2.80	Medium sand with powder brownish yellow	siMSa
		3	3.04	Powder brown	Si
			3.22	Medium sand with fine sand yellow	fsaMSa
		4	4.10	Medium sand with powder brownish yellow	siMSa
			4.22	Medium sand with powder light brown	siMSa
			4.35	Powder brown	Si
			4.50	Medium sand with powder brownish yellow	siMSa
			4.70	Powder brown	Si
		5	4.88	Medium sand with powder light brown	siMSa

Fig. 1. Geological cross-section profile photo in the audited profile [5]

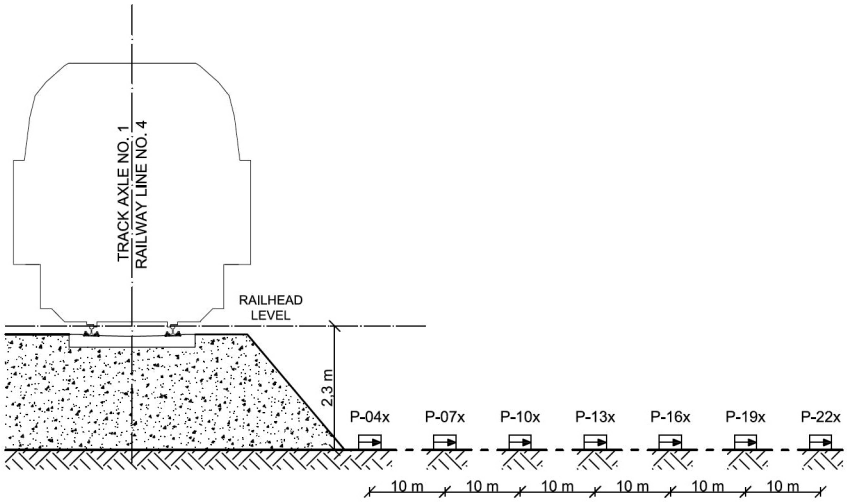

Fig. 2. Schematic arrangement of sensors in the measuring profile

3. Analysis of the acceleration records

All records were analysed. Summaries of the record for the speed of 160 km/h of the Pendolino train and a train of the Intercity type are shown in Fig. 3 and Fig. 4, respectively. For each of the passages of the trains, we imposed records of the horizontal component *x* of vibration measured at the points P-04*x* – P-22*x*. The maximum displacements of timelines achieve much lower values during the passage of the Pendolino; sensor placed under the embankment (P-04*x*) records the maximum acceleration not exceeding 70 cm/s^2, while extreme acceleration caused by passing through the InterCity rolling stock is more than twice the size and reaches values of up to 150 cm/s^2. In both cases, one can observe very high damping, particularly evident between the first and second sensor (a distance of 10 m).

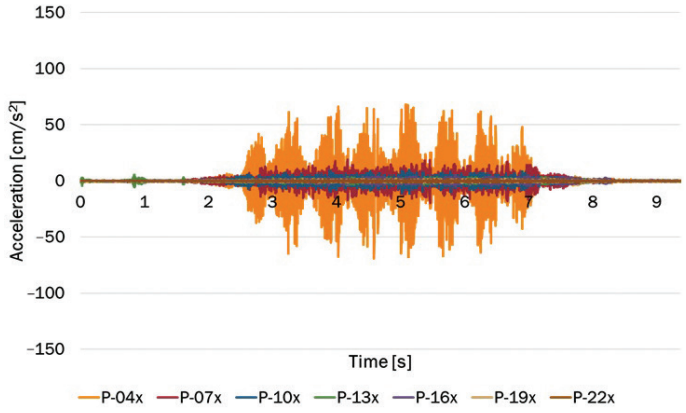

Fig. 3. Record of the horizontal component *x* of free-field vibrations caused by passing the Pendolino train at *v* = 160 km/h

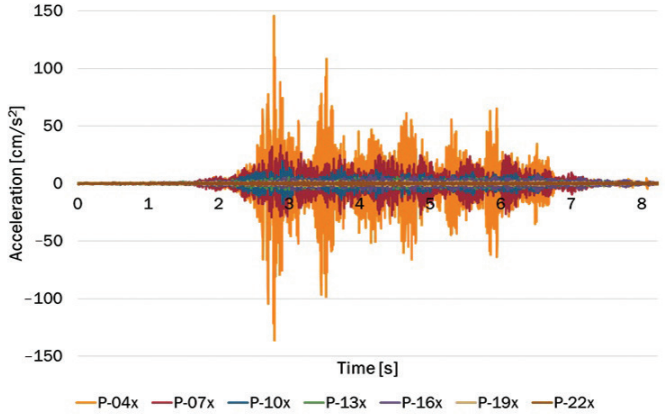

Fig. 4. Record of the horizontal component *x* of free-filed vibrations caused by passing the Intercity train at *v* = 160 km/h

Table 1 shows the maximum values obtained from the records of horizontal component x of free-field vibrations caused by passages of the Pendolino and InterRegio trains with a speed of 120 km/h and passages of the one Pendolino and four InterCity trains with a speed of 160 km/h. For passages of up to 120 km/h, only at the measuring point P-07*x*, slightly higher maximum values of vibration acceleration for the Pendolino train were recorded. In the other six points of the measurement, lower maximum acceleration vibration, caused by passing that trains, was recorded. At a speed of 160 km/h, a very large discrepancy in the results of maximum acceleration values of the horizontal component *x* of free-field vibrations can be seen due to passages of the same carrier (InterCity); at P-04*x*, a difference of up to 50 cm/s^2 is observed. During EMU 250 passages, the lowest intensity of free-field vibrations was registered at each measuring point.

Table 1

Statement of the maximum value of the horizontal component of free-field vibrations

Source of vibration	Measuring point number						
	P-04*x*	P-07*x*	P-10*x*	P-13*x*	P-16*x*	P-19*x*	P-22*x*
Pendolino 120 km/h track A – 12:50	81.11	14.1	4.92	2.75	2.24	1.27	0.99
InterREGIO 120 km/h track A – 11:50	85.93	12.55	7.54	3.78	2.61	1.82	1.18
Pendolino 160 km/h track A – 13:49	68.88	19.73	10.74	5.79	5.27	2.08	1.34
Intercity 160 km/h track A – 12:33	96.81	33.52	18.05	7.07	7.02	2.85	2.08
Intercity 160 km/h track A – 14:04	98.17	35.81	18.03	6.57	6.8	2.55	2.29
Intercity 160 km/h track A – 13:28	112.02	19.66	8.55	5.22	3.66	2.64	1.54
Intercity 160 km/h track A – 10:12	145.8	33.09	19.21	5.95	7.96	2.55	2.35

Figure 5 shows decay curves of the maximum values of vibration acceleration with distance when traveling the Pendolino and the InterREGIO trains at a speed of 120 km/h. For each set of data, there is a power function given. It describes the dependence of the maximum acceleration of the distance from the vibration source. The coefficients of determination R^2 for both functions is approximately 0.99. The maximum values of vibration acceleration did not show significant differences between the Pendolino and InterRegio train journeys.

Figure 6 summarises the maximum values of horizontal component *x* of free-field vibrations caused by trains passages at a speed of 160 km/h (one Pendolino and four InterCity trains). Next, the maximum acceleration values obtained from passages of InterCity were averaged. The values obtained from the Pendolino passes and averaged passages

from the InterCity are shown in Figure 7. The proposed power function describes well the disappearance of the maximum values of the horizontal component *x* of free-field vibrations with distance – the coefficient of determination R^2, respectively, 0.97 and 0.98. For the first three accelerometers (P-04*x* P-07*x* and P-10*x*), it clearly shows much larger maximum vibration acceleration values obtained from passages of InterCity trains. The difference very quickly dissapears with distance and the fourth measurement point (P-13*x*) is practically invisible.

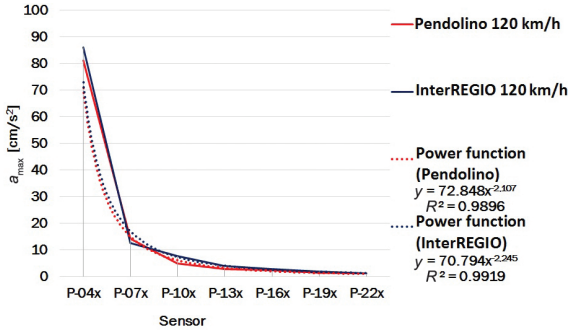

Fig. 5. The maximum value of the horizontal component *x* of free-field vibrations from the recorded accelerations caused by trains at a speed of *v* = 120 km/h

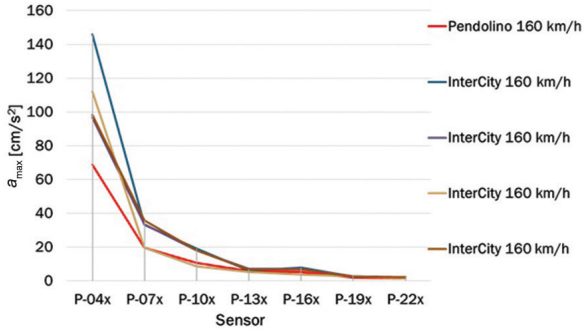

Fig. 6. The maximum value of the horizontal component *x* of free-field vibrations from the recorded accelerations caused by trains at a speed of *v* = 160 km/h

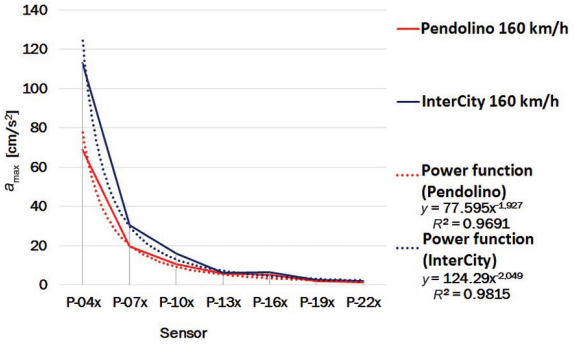

Fig. 7. The maximum value of the horizontal component *x* of free-field vibrations from the recorded accelerations caused by trains at a speed of *v* = 160 km/h

4. Vibration spectrum analysis

The recorded free-field vibrations were analysed using one-third octave band frequency filters, and distributed in one-third octave bands of the mid-band frequency from 1 to 100 Hz. For example, Fig. 8 and 9 summarise the results of the horizontal component *x* of free-field vibrations recorded at the measurement point P-04*x* from various trains passages at speeds of $v = 160$ and 120 km/h. In both cases, a band of less than 16 Hz shows almost zero acceleration for each of the rolling stock. A distinction can be made only in the bands from 16 to 100 Hz.

Comparing the maximum value of the horizontal component *x* free-filed vibrations in one-third octave bands, caused by passing InterCity trains and EMU 250, shows that newly purchased trains inspire some of the lowest vibration accelerations in all third octave frequency bands. Comparing the acceleration values in each one-third octave bands of excited Pendolino trains crossing and InterREGIO cannot clearly identify rolling stock generates less vibration acceleration. In the range of 16–50 Hz, EMU 250 generates a lower level of acceleration, which changes in the higher frequency band (63 to 100 Hz).

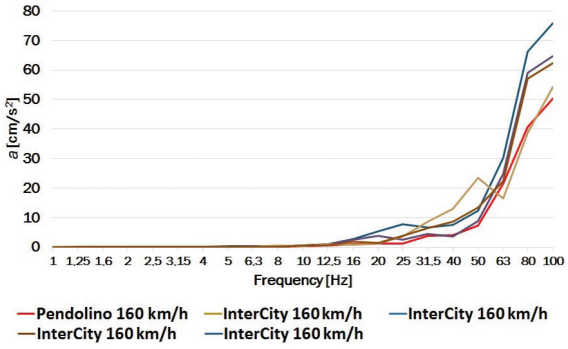

Fig. 8. Vibration spectrum in third octave frequency bands – the measuring point P-04*x* – speed trains $v = 160$ km/h

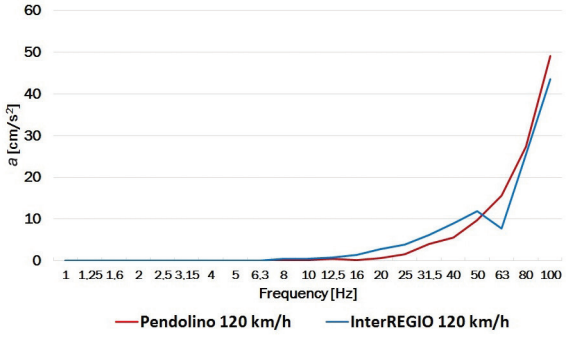

Fig. 9. Vibration spectrum in third octave frequency bands – the measuring point P-04*x* – speed trains $v = 120$ km/h

5. Continuous spectrum of vibrations

Using Fast Fourier Transform (FFT), the transition from the time domain to the frequency domain was performed to yield a continuous vibration spectrum. Transform was performed for frequencies of up to 100 Hz. Figure 10 illustrates the change of the frequency spectrum depending on the distance of the measuring point from the source of the vibration for the InterCity train. For the first measurement point (P-04*x*), higher vibration frequencies are dominant – range from 63 to 100 Hz. However, frequencies from the range 70–75 Hz for a sensor at a distance of 10 m (P-07*x*) dominate, reaching the maximum value equalling the values obtained at the measuring point P-04*x* in that band. Also, in the 70–75 Hz range of maximum acceleration values at the third (P-10*x*) and fourth (P-13*x*) measuring point, but these values are much smaller compared with the values obtained based on the records in the first (P-04*x*) and the second (P-07*x*) measurement point. In order to make better visualisation, the frequency spectrum is divided into a bandwidth of 3 Hz and average amplitude of the vibrations is calculated. Maps figure showing the obtained value of the acceleration from the frequency and distance of the sensor from the source of the vibration is shown in Fig. 11. The largest amplitude of the vibrations occurs in the first measuring point (P-04*x*) and corresponds to higher frequency bands, but the band of 66–72 Hz is a band in which there is the slightest damping with increasing distance from the source of vibration. The amplitudes greater than 0.1 cm/s^2 are transferred up to 40 meters from the embankment (fifth measuring point – P-16*x*).

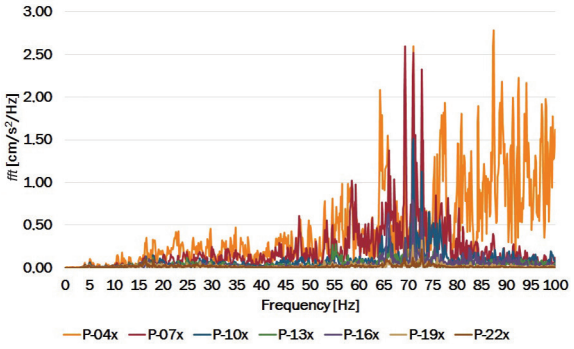

Fig. 10. Continuous vibration spectrum – InterCity train – velocity v = 160 km/h

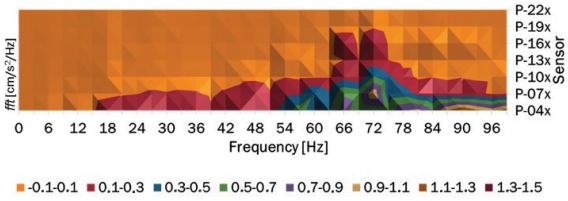

Fig. 11. Map propagation of vibration – InterCity train – velocity v = 160 km/h

To determine the frequency bands with the greatest damping of a continuous spectrum, we calculated the relation of the spectrum from record at the last sensor (P-22*x*) to the spectrum from the first sensor (P-04*x*). The calculated dependence is shown in Figure 12. Although the expected values should be less than 1.0, taking into account the decay of vibration with distance from the source, approx. 2% of the resulting relationship exceeds this value. It was not due to the presence of very large amplitudes of vibration on the last sensor (P-22*x*) and only very small values of records of vibration acceleration in the first measurement point (P-04*x*). This is not also the fact that the signals at these frequencies were strengthened. This was probably caused by changes in signal frequency resources after passing through a very heterogeneous material, which is ground.

In order to better visualise the damping, Figure 13 shows the same relationship, but after the removal of excess 1. Here, we can see that the greatest attenuation corresponds to the highest frequencies, which is in line with expectations.

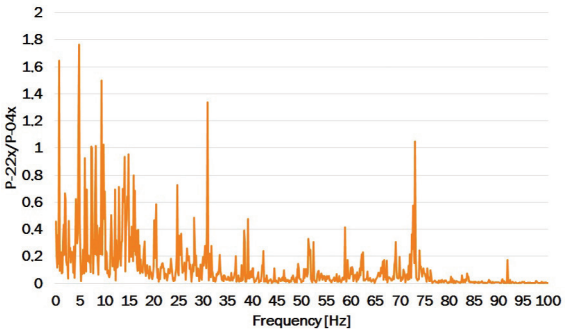

Fig. 12. The ratio of vibration spectrum transmitters P-22*x* and P-04*x* – Intercity train – the speed of 160 km/h

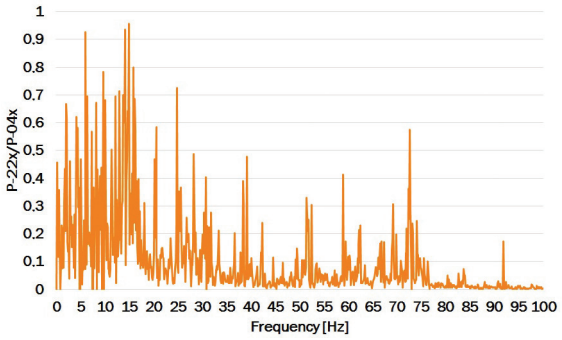

Fig. 13. The ratio of vibration spectrum transmitters P-22*x* and P-04*x* after verification – Intercity train – the speed of 160 km/h

Similarly as for the InterCity train, we examined continuous spectrum of free-field vibrations excited by passages of the Pendolino train at a speed of 160 km/h. Vibration spectrum and map of acceleration amplitudes induced by passages of the InterCity and the Pendolino train are shown in Fig. 14 and 15, respectively.

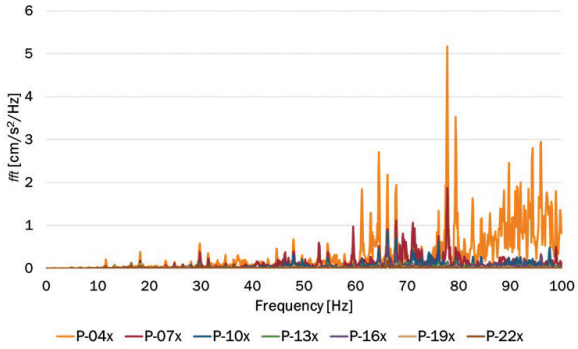

Fig. 14. Continuous vibration spectrum – Pendolino train – velocity v = 160 km/h

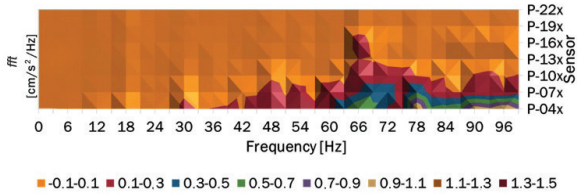

Fig. 15. Map propagation of vibration – InterCity train – velocity v = 160 km/h

Similarly, for EMU 250, the dominating frequencies of the recorded horizontal component x free-field vibrations are in the first measurement point (P-04x) and occur in the band with the highest frequencies. However, the bandwidth that is the least damped is a band with a centre frequency of 66 Hz.

Similarly as for the InterCity train, we compared the continuous spectrum of vibrations recorded at the last measuring point (P-22x) with the spectrum of the vibration record from the first measuring point (P-04x) – dependence is shown in Figure 16. The composition of the Pendolino, approx. 1.5% of the value exceeded the value of 1. Ratio spectra after the removal of greater than 1 are shown in Figure 17. As in the case of Intercity – see Fig. 13, an increase of damping can be observed with an increase of the frequency.

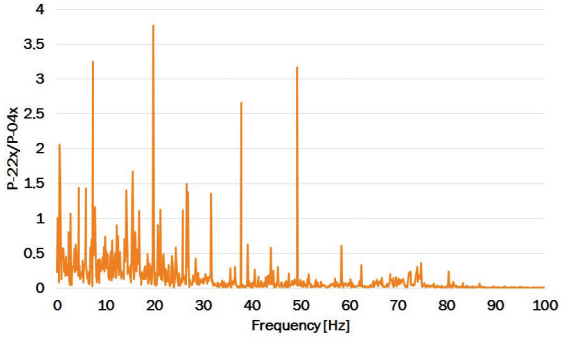

Fig. 16. The ratio of vibration spectrum for records from measurement point P-22x and P-04x – Pendolino train – the speed of 160 km/h

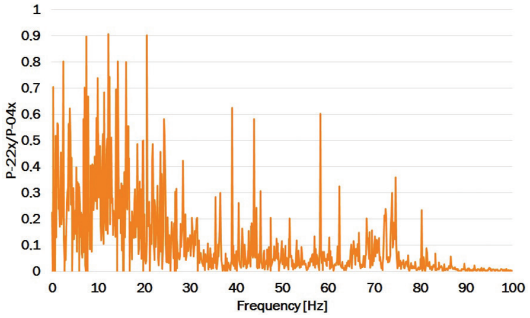

Fig. 17. The ratio of vibration spectrum for records from measurement point P-22*x* and P-04*x* –Pendolino train – the speed of 160 km/h – after verification

6. Analysis of vibration velocity

A continuous spectrum obtained by means of Fast Fourier Transform was used to calculate the free-field velocity. Using the formula for harmonic vibrations, integral formulae and amplitudes of vibration acceleration, we calculate the approximate values of velocity amplitudes [4].

The amplitudes of velocities were calculated for a frequency of 0.5–100 Hz. In both cases (vibration induced by passages of the old and new rolling stock), values of velocity amplitudes calculated at the measurement point under the embankment (P-04*x*) clearly exceed the values obtained at other measuring points, but there is a single frequency for which these velocity are smaller. The decrease in the values of velocity, depending on the distance, is not linear. Distribution of free-filed velocity vibration in frequency domain – the InterCity train – velocity $v = 160$ km/h for both kind of trains are shown in Fig. 18 and Fig. 19.

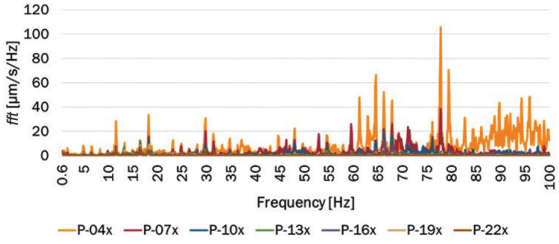

Fig. 18. Distribution of free-filed velocity vibration in frequency domain – the Pendolino train – velocity $v = 160$ km/h

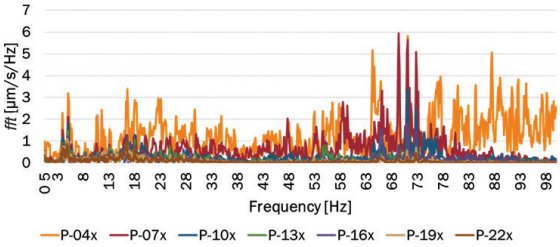

Fig. 19. Distribution of free-filed velocity vibration in frequency domain – the InterCity train – velocity $v = 160$ km/h

7. Analysis of vibration displacements

A continuous spectrum obtained by means of Fast Fourier Transform was used to calculate free-field displacement. Using the formula for harmonic vibrations, integral formulae and amplitudes of vibration acceleration, we calculated the approximate values of displacement amplitudes [4].

The amplitudes of displacements were calculated for a frequency of 0.5–100 Hz. Due to the very small displacement values (maximum value is less than 0.1 microns) for high frequencies, the charts show only the values in the frequency range of 0.5–2 Hz (amplitude of displacements exceeds 0.1 μm). In both cases (vibration induced by passages of the old and new rolling stock), values of displacement amplitudes calculated at the measurement point under the embankment (P-04*x*) clearly exceed the values obtained at other measuring points, but there is a single frequency for which these displacements are smaller. Although the distance between successive sensors is the same – a sharp decline in free-filed vibration displacements is not observed. The decrease in values of displacements depending on the distance is not linear. The calculated distribution of free-field displacement vibration in frequency domain for both kinds of trains are shown in Fig. 20 and Fig. 21.

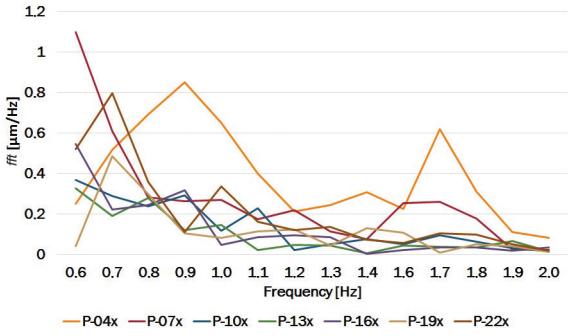

Fig. 20. Distribution of free-filed displacement vibration in frequency domain – the Pendolino train – velocity v = 160 km/h

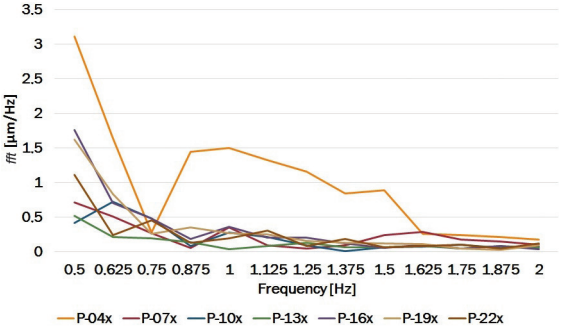

Fig. 21. Distribution of free-filed displacement vibration in frequency domain – the InterCity train – velocity v = 160 km/h

8. Conclusions

Railway line no. 4 (CRL), which is the "backbone" of high-speed rail in Poland, cannot allow speed limits because of vibration. Surface and rolling stock have to be designed so as to standard limits the propagation of vibration was not exceeded while enhancing the speed of rolling stock on the entire length of the line.

Operation of the Pendolino train in Poland will improve the "climate vibration" of railway lines. Based on measured and calculated values, decay curves of free-field vibrations, depending on the distance from the source of vibration, were analysed.

The designated frequency spectrum of the vibration records allowed to determine the dominant frequency bands and to compare them for different trains and ride speed. The results of the analysis indicated that travel at the speed of v = 160 km/h, the Pendolino attracted lower values of vibration acceleration compared to the InterCity train. On the other hand, when traveling by the InterRegio train (v = 120 km/h), for frequency f = 50 Hz, the induced vibration level was higher than in the EMU 250. For higher frequency bands, the Pendolino attracted a slightly higher level of vibration.

Another aspect is very large spread in the results obtained by the InterCity. This is due to the heterogeneity of rolling stock, which is associated with the technical condition of the different configurations. In order to improve the environmental conditions, this would limit the exploitation appropriate traction units, not the number of trips generally performed by all trains.

The displacement values were analysed and calculated based on the recorded vibration acceleration. Analysis of displacements in a band of frequency up to 2 Hz indicates that they rapidly decay with distance.

High speed trains are not an end in themselves, but only a means to achieve this objective, which is e.g. faster movement between towns, and improvement of comfort and quality of life of the user turn. However, improving the comfort of one man (here the passenger) cannot be at the expense of worsening the living conditions of the other (here people living in areas in the neighbourhood of railway lines). Therefore, aspirations to build high-speed rail cannot ignore the environmental aspects.

References

[1] Degrande G., Schillemans L., *Free field vibrations during the passage of a Thalys high-speed train at variable speed*, Journal of Sound and Vibration 247(1)/2001, 131–144.

[2] Tompson D., *Railway noise and vibration, Mechanisms, Modelling and Means of Control*, Institude of Sound and Vibration Research University of Southampton, UK, Elsevier, 2009.

[3] Lawrance T., *Noise and vibration from road and rail*, CIRIA, London 2011.

[4] Krylov V.V., *Noise and vibration from high-speed trains*, Thomas Telford, Londyn 2001.

[5] Pilecka E., Pietras J.S., Zięba J., Morman J., Przydatek P., *Dokumentacja badań podłoża dla zadania: Wstępne rozpoznanie warunków gruntowych w punktach pomiarowych dynamicznego oddziaływania składu Pendolino na otoczenie*, Praca własna Zakładu Współdziałania Budowli z Podłożem, Instytut Mechaniki Budowli, Wydział Inżynierii Lądowej, Politechnika Krakowska, archiwum, Kraków 2013.

[6] Stypuła K., Tatara T., *Wybrane wyniki pomiarów drgań wywołanych testowymi przejazdami pociągu Pendolino na CMK*, [in:] Materiały IX Seminarium Wpływ hałasu i drgań wywołanych eksploatacją transportu szynowego na budynki i ludzi w budynkach: diagnostyka i zapobieganie, Wibroszyn 2014, Politechnika Krakowska, Kraków 2014, 37–50.

[7] Maciąg E., Chełmecki J., Tatara T., *Badania gruntu i niskich budynków od wpływu komunikacji miejskiej*, Inżynieria i budownictwo 3/2005, 135–140.

[8] Ciesielski R., Kwiecień A., Stypuła K., *Propagacja drgań w warstwach przypowierzchniowych podłoża gruntowego*, Badania doświadczalne in situ, Politechnika Krakowska, Kraków 1999.